Published in final edited form as:
Clin Orthop Relat Res. 2005 July ; (436): 81–90.

Patellofemoral Joint Biomechanics and Tissue Engineering

Gerard A. Ateshian, PhD and **Clark T. Hung, PhD**
Columbia University, New York, NY

Abstract

Recent advances in the study of patellofemoral joint biomechanics have provided promising diagnosis and treatment modalities for patellofemoral joint disorders, such as quantitative assessment of cartilage lesions from noninvasive imaging, computer simulations of surgical procedures for optimizing surgical parameters and potentially predicting outcomes, and cartilage tissue engineering for the treatment of advanced degenerative joint disease. These technologies are still in development and their clinical potentials remain an ongoing topic of investigation. We review some of our progress in addressing these issues, and the important role of cartilage mechanics and lubrication in understanding the challenges regarding patellofemoral surgery and cartilage tissue engineering.

Studies of patellofemoral joint (PFJ) biomechanics traditionally have focused on force analysis, joint kinematics, and articular contact forces, areas and stresses. These studies have yielded valuable insight that is applied routinely in the clinical treatment of patellofemoral joint disorders.[2, 3, 13, 27, 37, 47, 48] For example, one of the motivations for tibial tuberosity transfer in patients with patellar malalignment is to reduce contact forces and stresses at the articulation, to alleviate pain, and to restore function.[39, 62, 63] As new technologies have developed, such as noninvasive imaging of cartilage layers with magnetic resonance imaging (MRI), it has become possible to asses the precise distribution of cartilage thickness in patients who have been diagnosed with osteoarthritis (OA).[22, 26, 29, 43, 49] Advance knowledge of this cartilage thickness distribution may be helpful in planning for patellar realignment surgery because it may be possible to anticipate whether the shift in articular contact areas after surgery will produce weightbearing on thicker or thinner cartilage.[24] Because the cartilage thickness distribution may vary considerably among healthy and arthritic patients, quantitative methods for identifying regions of abnormal cartilage thinning would be valuable.[26]

Computer modeling of diarthrodial joints also has evolved considerably in recent years, and it has now become possible to simulate certain surgical procedures using physics-based models derived from patient-specific imaging data.[11, 18, 24, 28, 32, 38, 71, 82, 83] Such simulations may help identify further the likely alteration in patellofemoral joint kinematics and articular contact after surgery. In patients with advanced OA however, realignment procedures alone may not be sufficient for achieving successful outcomes, and joint replacement also may be necessary. Cartilage tissue engineering, an emerging field in medicine, might be a promising alternative to artificial joints, wherein defects in the articular surface my be filled with cells [70, 103] or tissue grown in vitro.[35, 84, 90, 93] A potential long-term alternative to artificial joint replacement is the engineering of anatomically shaped tissue constructs which can replace the entire articular surface of the patella or femoral trochlea.[51, 52] For such procedures to be successful, it is essential to understand the

Correspondence to: Gerard A. Ateshian, PhD, Columbia University, 500 West 120th St, MC 4703, 220 S.W. Mudd, New York, NY 10027. Phone: 212-854-8602; Fax: 212-854-3304; ateshian@columbia.edu.

mechanical demands on these constructs and the need to reproduce the mechanical and frictional properties of native tissue.

We review our progress in characterizing the three-dimensional geometry of the articular layers of normal and osteoarthritic patellofemoral joints, using magnetic resonance imaging.[25, 26] By reporting specific applications, we show that knowledge of the cartilage thickness distribution may be useful not only for identifying articular lesions non-invasively [26], but also for simulating tibial tuberosity transfer surgery whose aim is to shift contact areas and stresses to more healthy regions of the articular layers.[24] For patients with advanced PFJ osteoarthritis however, such surgical procedures may be inadequate and one alternative to arthroplasty is to implant engineered cartilage whose mechanical and frictional properties match those of normal native tissue.[52, 65, 66] A review of the salient biomechanical properties of normal tissue is thus provided to help guide the design objectives for cartilage tissue engineering.[8, 57, 58] The loop is then closed by demonstrating that the three-dimensional articular surface topography acquired from imaging can be used with computer-aided design methodologies to generate articular layers in the shape of the human patella. [51, 52] Thus, the aim of this review is to demonstrate how various engineering methodologies can be integrated comprehensively with the purpose of advancing treatment modalities for PFJ disorders.

Cartilage Layer Geometry and Thickness

The three-dimensional articular layer geometry of the human patellar and distal femoral surfaces has been quantified using cryosectioning [98, 102], stereophotogrammetry [7, 41, 50], A-mode ultrasound [1] and magnetic resonance imaging (MRI) [19, 25, 29, 92]. Authors of these studies have shown that the cartilage layers of the patella and distal femur are nonuniform across the articular surface. In the patella, the cartilage is thicker along the mid-horizontal plane, with the peak thickness on the lateral facet, whereas in the femur, cartilage is thickest in the trochlea, followed by the lateral condyle [26, 49]. The average cartilage thickness distribution in the patella and femur is shown on thickness maps (Fig 1) from a study by Cohen et al,[26] obtained from 14 normal joints. For these normal templates, the reported surface-wide average thickness was 2.2±0.4 mm for the femur and 3.3±0.6 mm for the patella, with peak values of 3.7 mm and 4.6 mm, respectively. More detailed values of the cartilage thickness in different compartments of the knee are presented by Hudelmaier et al[49], classified by gender for young and elderly patients.

The ability to measure cartilage thickness and volume noninvasively with magnetic resonance imaging has made it possible to investigate these measures in patients with patellofemoral joint OA [20, 21, 40, 43, 81, 87]. In a study of 31 patients, Cohen et al[26] reported the average cartilage thickness distributions in 33 patellofemoral joints in patients with OA (Fig 2A) and compared them with the normal templates (Fig 1). The resulting “difference” maps provided an intuitive visual assessment of the distribution of cartilage loss across the articular surfaces of the patellofemoral joint (Fig 2B). These results confirmed that, on average, cartilage loss in patellofemoral joint OA occurs predominantly on the lateral facet of the patella, and to a lesser extent, on the lateral trochlea. Even though patients were diagnosed primarily with patellofemoral joint OA, cartilage loss on the femur was greater in the condyles than in the trochlea, with the greatest loss on the medial condyle (Fig 2B). These results help to support the hypothesis that patellofemoral joint OA rarely is isolated from tibiofemoral joint OA. The methodologies Cohen et al[26] developed in this study also can be applied to identify cartilage lesions in an individual patient.

Biomechanical Analyses and Surgical Simulations

Noninvasive imaging of cartilage layers with MRI also has been used to determine patellofemoral joint kinematics and articular contact areas in situ, at various angles of knee flexion, under load bearing [25, 42, 44, 72, 80, 89]. Although techniques for in vivo measurements of contact areas are still in development, results to date suggest good agreement with earlier in vitro studies on cadaveric joints [2, 3, 37, 47, 48, 101].

The benefits of anatomic reconstructions from MRI can be extended to the creation of physics-based models of diarthrodial joints, which then can be used in biomechanical analyses and surgical simulations [11, 18, 24, 28, 32, 38, 71, 82, 83]. In a study of 20 patients with patellofemoral joint OA, Cohen et al[24] created patient-specific models of the knee from MRI data (Fig 3A). Using these models, simulations of tibial tuberosity transfer surgery were done (Fig 3B) for various amounts of anteriorization and medialization. The models were used to predict articular contact areas and stresses, taking into account the patient-specific variation in articular thickness. Cohen et al[24] showed that the mean contact stress decreased in the knee models of most patients after surgical simulation, although the outcomes were not always consistent. In 85% of patients, all four simulated surgeries produced a decrease in the mean contact stress; in the remaining 15% at least one of the surgical simulations led to an increase in stress. On average, the greatest decrease in stress occurred with 20 mm anteriorization (−17%), followed by 15 mm anteriorization (−15%), 15 mm anteriorization + 8 mm medialization (−14%), and 8 mm anteriorization + 8 mm medialization (−9%). Similarly, medialization of the patellar tendon insertion led to a substantial medial shift in the centroid of the contact area: a 4.4 mm shift with 8 mm medialization, and a 3.8 mm shift with 15 mm medialization. The counterintuitive finding of smaller medial shift in the contact centroid with greater medialization of tibial tuberosity reflects the interaction between complex articular surface geometry and contact mechanics. The average reductions in contact stress magnitude were statistically significant but seem relatively modest from a contact mechanics perspective. These types of surgical simulations remain to be validated in prospective clinical studies, which would establish whether patient-specific biomechanical outcomes obtained from such simulations correlate with clinical outcomes such as joint pain.

Cartilage Mechanics and Lubrication

One of the major factors implicated in cartilage degeneration is the magnitude of stresses and strains within the articular layers during contact loading. In posttraumatic OA, progressive joint degeneration is attributed, at least in part, to the initial mechanical failure of the tissue under excessive contact stresses [12, 31, 53, 69, 85, 100]. However, the magnitude of contact stresses alone does not determine the magnitude of stresses and strains within the collagen-proteoglycan solid matrix of cartilage. The loading history (the rate of change and duration of applied contact stresses) and the mechanical properties of articular cartilage are essential factors that control the tissue's ability to sustain its loading environment or fail under pathologic conditions.

Articular cartilage has high water content, ranging from 65 to 90% of the tissue weight, depending on age and location throughout the thickness of the articular layer. This water can flow within the porous-permeable collagen-proteoglycan matrix, albeit with great resistance because of the low permeability of the solid matrix. When cartilage is compressed, this interstitial fluid will pressurize considerably and contribute to supporting the applied contact stress [68, 75, 104]. If the stress is maintained constant the interstitial fluid pressure slowly subsides as the water flows away from the loaded regions, while the solid matrix deformation increases. Eventually, the tissue response reaches equilibrium, with no further change in deformation or strain with time. This time-dependent response, called flow-

dependent viscoelasticity, has been successfully modeled by the biphasic theory of Mow et al.[74] This theory relies on measurements of the mechanical properties of the solid matrix under equilibrium conditions and the permeability of the matrix to interstitial fluid flow.

The biphasic properties of human patellofemoral joint cartilage have been reported by several investigators [4, 5, 30, 36, 58]. For example, Krishnan et al[58] determined the tensile and compressive moduli and radial and axial permeabilities of the solid matrix as a function of depth from the articular surface to the deep zone (Fig 4). As observed in the articular layers of other joints [54, 91], the tensile modulus of patellar and femoral cartilage decreases from the superficial to the deep zone whereas the compressive modulus increases.

It has long been known from experimental measurements that the tensile modulus of cartilage is significantly greater (by up to two orders of magnitude) than its compressive modulus. Because the primary mode of loading of articular cartilage is in compression, the significance of this counterintuitive finding was poorly understood until recently. From studies in which the biphasic theory was extended to account for the disparity in tensile and compressive properties [23, 94, 97], we now understand that the high tensile modulus of cartilage considerably constrains its lateral expansion under axial compressive loading. Because the water and solid matrix of cartilage are nearly incompressible, the great resistance to lateral expansion under axial loading produces highly elevated interstitial fluid pressurization within the cartilage. This elevated fluid pressure contributes to supporting more than 90% of the applied contact stress at the articular surface in the short-term response of cartilage to loading [6, 60], increasing the dynamic stiffness of cartilage in compression [46, 55, 78, 88].

These theoretical predictions have been verified experimentally [77, 79, 95, 96]. For example, in our study [79], the fraction of the load supported by interstitial fluid pressurization was measured in unconfined compression stress-relaxation in human patellar and femoral cartilage and bovine calf femoral cartilage. At the articular surface, the fluid load support was 79±11% in human tissue and 94±4% in calf tissue; at the deep zone, where the disparity in tensile and compressive properties is smaller (Fig 5), the respective values were 69±15% and 71±8%. The smaller magnitude of fluid load support observed at the articular surface of human adult cartilage, compared with immature bovine cartilage, could be a reflection of a greater degree of degradation.

Using their experimentally-measured properties of human patellar and femoral cartilage (Fig 4), Krishnan et al[58] did a biphasic finite-element analysis simulating articular layer contact. They found that the peak stresses in the solid matrix of the articular layer were tensile, occurring at the articular surface, at the center of the contact region, and oriented in a direction tangential to the surface. The peak compressive stresses in the solid matrix were about 10 times smaller than the peak tensile stresses because most of the compressive load is supported by interstitial fluid pressurization. In contrast, the peak strains occurred at the cartilage-bone interface, away from the centerline of contact. These theoretic results help to understand two commonly observed modes of cartilage degradation or failure under loading: (1) surface fibrillation and vertical fissures, which occur at the articular surface after impact loading, may be explained by excessive tensile stresses in the tangential direction; (2) occult injuries at the cartilage-bone interface may be explained by excessive strains or shear stresses in the deep zone [9, 10]. These results allow us to emphasize the importance of the tensile properties of the superficial zone in sustaining the compressive loads applied across the joint.

In addition to increasing the dynamic stiffness of articular cartilage under compressive loading, interstitial fluid pressurization plays a crucial role in regulating its frictional

response. Because the primary function of articular cartilage is to act as a bearing material in diarthrodial joints, it is essential that friction and wear remain low under normal joint function. The friction coefficient of cartilage, which is the ratio of the friction force during sliding divided by the applied load, has been measured experimentally in numerous studies.[73] Although experiments have confirmed that the friction coefficient of cartilage can be very low (on the order of ~0.002–0.02), they also have shown that it increases with time under a constant applied load [34, 57, 61, 68]. The rate of increase matches the rate of cartilage creep deformation attributed to flow-dependent viscoelasticity, and the friction coefficient achieved under equilibrium conditions is much higher than that in the early-time response (~0.1–0.5). This equilibrium friction coefficient is far too elevated to provide efficient lubrication because the resulting frictional forces produce considerable wear over a relatively short period of time [33]. Therefore, one must presume that, under in vivo loading conditions, equilibrium conditions do not prevail and the friction coefficient remains in the lower range of experimentally measured values. Interestingly, only a few investigators have focused on this time-dependent increase in the friction coefficient, even though this behavior holds the key to understanding the mechanism of lubrication in diarthrodial joints.

McCutchen [68] proposed that the time-varying increase in the friction coefficient is caused by concomitant decrease in fluid pressurization. As long as the pressure remains high, most of the compressive load transmitted across the articular surfaces would be supported by the fluid, thereby minimizing the friction between the solid matrixes of apposing surfaces. As the pressure decreases and fluid flows away from the loaded region, the solid matrixes would support a greater share of the applied load, producing greater friction. With the insight gained from the validation of the biphasic theory for cartilage,[74] which can predict the mechanism of fluid pressurization, other investigators supported this hypothesized mechanism for cartilage lubrication [8, 34, 61]. Krishnan et al[57] provided direct experimental verification of this hypothesis by measuring the frictional response of cartilage simultaneously with its interstitial fluid load support (Fig 6). The linear negative correlation observed between these measured parameters agreed with Ateshian et al's[8] model, in which they formulated the dependence of the friction coefficient on interstitial fluid load support within the framework of biphasic theory.

The clinical significance of these results is that the frictional response of cartilage is governed only secondarily by synovial fluid lubricants [17, 45, 86, 99]. Because the friction coefficient remains low only as long as the interstitial fluid load support is high, the integrity of the cartilage layers is critical for maintaining low friction and wear. Any mechanism of tissue degradation (eg, fibrillation, chondromalacia, arthritis) that leads to a decrease in the tensile modulus relative to the compressive modulus of the tissue would result in a loss of interstitial fluid load support and increase in the friction coefficient. These findings suggest that intra-articular injections of hyaluronan in arthritic joints are not likely to reduce friction at the articular surfaces; any putative therapeutic effects of such injections would have to be attributed to other factors.

Tissue Engineering of Patellar Articular Layers

There are many challenges to engineering successful cartilage replacements. These include identifying suitable cell sources, media supplements, bioreactor design features, implantation procedures, postsurgical treatment, etc. Each of these challenges is critical to a successful tissue engineering strategy and progress toward this goal is advancing along these parallel tracks. The specific challenges addressed in functional tissue engineering studies [14, 52, 65, 66] are the importance of the mechanical properties and geometry of engineered cartilage constructs and strategies for successful implantation.

Because the load support and frictional mechanisms of cartilage are so intimately dependent on its mechanical properties and because cartilage has a limited ability for repair in situ, our strategy for engineering cartilage constructs has focused on reproducing the normal properties of native tissue under in vitro conditions before implantation [52]. One hypothesis is that dynamic loading of chondrocyte-seeded constructs can promote mechanical properties that approach those of native tissue [14, 56, 65]. In a study by Mauck et al,[65] cylindrical agarose gels seeded with primary bovine chondrocytes were subjected to dynamic loading in unconfined compression at 1 Hz, for 3 hours per day over a period of 4 weeks. A control group of cells was cultured under similar conditions, without loading. The equilibrium modulus of the constructs increased from 4.8±2.3 kPa at day 0 to 100±16 kPa for loaded constructs and 15±8 kPa for free-swelling controls at day 28. In comparison, the native tissue from which the cells were obtained has an equilibrium modulus of 277±83 kPa. The authors showed that dynamic loading can be effective for promoting better mechanical properties in engineered cartilage. One potential advantage of dynamic loading of cylindrical disks in unconfined compression is that this loading configuration promotes compressive strains in the axial direction and tensile strains in the radial and circumferential directions, similar to the native environment of articular cartilage.

In a subsequent study, Mauck et al[67] showed that tissue growth and its response to dynamic loading also was dependent on cell seeding density and nutrient supply. Mechanical properties improved considerably when increasing the cell seeding density from 10 million to 60 million cells per mL, and the nutrient supply from 10 to 20% fetal bovine serum. After 56 days in culture, the equilibrium modulus of constructs in the high cell seeding density and high nutrient supply group was 186±11 kPa in the dynamically loaded constructs and 85±15 kPa in the free-swelling controls. Therefore, the dynamically loaded constructs had a modulus equal to 2/3 of the native tissue. Similarly, the dynamic modulus at 1 Hz was 1.64±0.46 MPa in the dynamically loaded constructs and 0.87±0.09 MPa in the free-swelling controls. In comparison, in similar testing conditions, the native tissue has a dynamic modulus of 7.0±0.7 MPa. Interestingly, unlike the mechanical properties of the tissue constructs, glycosaminoglycan (GAG) content and collagen content were found to be the same in free-swelling and dynamically loaded samples. The authors suggest that ultrastructural matrix organization, and matrix products other than GAG and collagen may have a substantial influence on the tissue's mechanical properties.

The results of these studies are encouraging because they show the mechanical properties of tissue engineered constructs approaching those of native tissue. While simultaneously exploring alternative strategies to further improve mechanical properties of engineered constructs, such as growth factor supplementation [64] or dynamic hydrostatic pressurization,[15, 16] the challenge of implanting tissue constructs into osteoarthritic joints also has been considered. Because loss of cartilage in degenerative joint disease usually spans a large percentage of the articular surface (Fig 2B), one long-term strategy is to consider replacing the entire articular layer with an anatomically shaped tissue-engineered construct.[51] Authors have shown[51, 52] the feasibility of generating constructs in the shape of the human patella, using three-dimensional geometric data derived from stereophotogrammetric measurements. The basic approach is to create anatomically shaped molds using computer-aided design techniques to form chondrocyte-seeded gels into the desired shape (Fig 7). These constructs can maintain their original shape for several weeks in free-swelling culture even as the matrix elaborates.

To anchor anatomically shaped cartilage layers into the native subchondral bone of a joint, it may be necessary to engineer osteochondral constructs in which the cartilage layer already is anchored into a bony substrate. In our exploratory studies [51, 52, 59], bovine trabecular bone was machined into the shape of the subchondral bone surface of a human patella using a

computer-controlled milling machine. Chondrocyte-seeded agarose gel was cast into the trabecular space to form an anatomically shaped osteochondral construct (Fig 8A). These constructs were cultured for up to 35 days under free-swelling conditions, showing progressive elaboration of matrix products from the periphery to the center. With such large constructs, it becomes apparent that nutrient consumption and diffusion limitations pose a considerable challenge for uniform matrix development [76] as evidenced by the GAG distribution on histological sections (Fig 8B).

Discussion

Noninvasive imaging of the articular layers of the patellofemoral joint has made it possible to quantify the cartilage thickness and volume in healthy patients and in patients with OA. Quantitative techniques can help identify the location and extent of cartilage lesions by comparing a patient-specific thickness map against a normal thickness template. Such techniques may become useful clinically for tracking the progression of joint degeneration in patients. Some challenges exist for practical clinical implementation of these methodologies. For example, manual or semi-automated segmentation of the articular layers from MR images needs to be performed by trained technicians who are familiar with normal and pathological articular layer anatomy. In addition, uniform standards of image acquisition must be set to ensure appropriate quality control. Current efforts are under way by several investigators and companies to establish such standards and provide these services. Ultimately, the cost-effectiveness of these diagnostic modalities needs to be established by determining their impact on patient treatments and outcomes.

Our studies have also demonstrated that physics-based, patient-specific computer models of the patellofemoral joint can be created from MRI data and used to simulate surgical procedures such as tibial tuberosity transfer. When validated, these models potentially could be used to identify optimal parameters for surgery, such as the amount of medialization and anteriorization. More critically than for the case of cartilage thickness mapping, the effectiveness of these surgical simulation tools needs to be established from patient studies. If found to be suitably predictive, the cost-effectiveness of these procedures would also need to be investigated. Surgical simulations require 3D MR imaging of the afflicted joint, manual or semi-automated segmentation of the articular layers, bones, ligaments and tendons, and possibly muscle lines of action. The surgeon or a trained operator would need to perform the surgical simulations and translate the computational results into potential clinical outcomes. The added costs of surgical simulations would need to be outweighed by a significant improvement in actual outcomes.

In patients with advanced joint degenerative disease, arthroplasty currently is the main treatment modality. With advances in cartilage tissue engineering however, it may become possible to replace entire articular layers with tissue-engineered osteochondral constructs whose geometry can be derived from noninvasive imaging of the patient's normal contralateral joint or from a database of normal joint geometries. One of the many challenges of tissue engineering scientists is to develop constructs whose material properties match those of native articular cartilage because these properties are essential for maintaining normal function and lubrication. Our studies of cartilage tissue engineering have focused on the need to reproduce the material properties and geometry of the native tissue in order to optimize survival of the implant in vivo. In addition to these aims, other challenges remain on the road to a successful tissue engineering treatment procedure, the most notable of which is the identification of the source of cells for clinical applications. Autologous chondrocytes or mesenchymal stem cells may prove to be adequate, although more research is needed to determine the clinical feasibility of various tissue engineering strategies.

Acknowledgments

One or more of the authors received funding from the National Institute of Arthritis, Musculoskeletal and Skin Diseases of the National Institutes of Health (AR46532, AR43628, AR46568).

References

1. Adam C, Eckstein F, Milz S, et al. The distribution of cartilage thickness in the knee-joints of old-aged individuals -- measurement by A-mode ultrasound. Clin Biomech (Bristol, Avon). 1998; 13:1–10.
2. Ahmed AM, Burke DL. In-vitro measurement of static pressure distribution in synovial joints--Part I: Tibial surface of the knee. J Biomech Eng. 1983; 105:216–225. [PubMed: 6688842]
3. Ahmed AM, Burke DL, Yu A. In-vitro measurement of static pressure distribution in synovial joints--Part II: Retropatellar surface. J Biomech Eng. 1983; 105:226–236. [PubMed: 6632824]
4. Akizuki S, Mow VC, Muller F, et al. Tensile properties of human knee joint cartilage: I. Influence of ionic conditions, weight bearing, and fibrillation on the tensile modulus. J Orthop Res. 1986; 4:379–392. [PubMed: 3783297]
5. Armstrong CG, Mow VC. Variations in the intrinsic mechanical properties of human articular cartilage with age, degeneration, and water content. J Bone Joint Surg Am. 1982; 64:88–94. [PubMed: 7054208]
6. Ateshian GA, Lai WM, Zhu WB, Mow VC. An asymptotic solution for the contact of two biphasic cartilage layers. J Biomech. 1994; 27:1347–1360. [PubMed: 7798285]
7. Ateshian GA, Soslowsky LJ, Mow VC. Quantitation of articular surface topography and cartilage thickness in knee joints using stereophotogrammetry. J Biomech. 1991; 24:761–776. [PubMed: 1918099]
8. Ateshian GA, Wang H, Lai WM. The role of interstitial fluid pressurization and surface porosities on the boundary friction of articular cartilage. J Tribology. 1998; 120:241–251.
9. Atkinson TS, Haut RC, Altiero NJ. Impact-induced fissuring of articular cartilage: an investigation of failure criteria. J Biomech Eng. 1998; 120:181–187. [PubMed: 10412378]
10. Atkinson TS, Haut RC, Altiero NJ. An investigation of biphasic failure criteria for impact-induced fissuring of articular cartilage. J Biomech Eng. 1998; 120:536–537. [PubMed: 10412426]
11. Benvenuti JF, Rakotomanana L, Leyvraz PF, et al. Displacements of the tibial tuberosity. Effects of the surgical parameters. Clin Orthop. 1997:224–234. [PubMed: 9345228]
12. Borrelli J Jr. Ricci WM. Acute effects of cartilage impact. Clin Orthop. 2004:33–39. [PubMed: 15232423]
13. Brechter JH, Powers CM. Patellofemoral joint stress during stair ascent and descent in persons with and without patellofemoral pain. Gait Posture. 2002; 16:115–123. [PubMed: 12297253]
14. Butler DL, Goldstein SA, Guilak F. Functional tissue engineering: the role of biomechanics. J Biomech Eng. 2000; 122:570–575. [PubMed: 11192376]
15. Carver SE, Heath CA. Increasing extracellular matrix production in regenerating cartilage with intermittent physiological pressure. Biotechnol Bioeng. 1999; 62:166–174. [PubMed: 10099526]
16. Carver SE, Heath CA. Semi-continuous perfusion system for delivering intermittent physiological pressure to regenerating cartilage. Tissue Eng. 1999; 5:1–11. [PubMed: 10207185]
17. Charnley, J., editor. Symposium on Biomechanics. London: Inst of Mech Engrs; 1959. The lubrication of animal joints; p. 12-22.
18. Cheng CK, Yao NK, Liu HC. Surgery simulation analysis of anterior advancement of the tibial tuberosity. Clin Biomech (Bristol, Avon). 1995; 10:115–121.
19. Cicuttini F, Forbes A, Morris K, et al. Gender differences in knee cartilage volume as measured by magnetic resonance imaging. Osteoarthritis Cartilage. 1999; 7:265–271. [PubMed: 10329301]
20. Cicuttini F, Wluka A, Wang Y, Stuckey S. The determinants of change in patella cartilage volume in osteoarthritic knees. J Rheumatol. 2002; 29:2615–2619. [PubMed: 12465162]
21. Cicuttini FM, Wluka AE, Hankin J, Stuckey S. Comparison of patella cartilage volume and radiography in the assessment of longitudinal joint change at the patellofemoral joint. J Rheumatol. 2004; 31:1369–1372. [PubMed: 15229959]

22. Cicuttini FM, Wluka AE, Stuckey SL. Tibial and femoral cartilage changes in knee osteoarthritis. Ann Rheum Dis. 2001; 60:977–980. [PubMed: 11557657]
23. Cohen B, Lai WM, Mow VC. A transversely isotropic biphasic model for unconfined compression of growth plate and chondroepiphysis. J Biomech Eng. 1998; 120:491–496. [PubMed: 10412420]
24. Cohen ZA, Henry JH, McCarthy DM, Mow VC, Ateshian GA. Computer simulations of patellofemoral joint surgery: Patient-specific models for tuberosity transfer. Am J Sports Med. 2003; 31:87–98. [PubMed: 12531764]
25. Cohen ZA, McCarthy DM, Kwak SD, et al. Knee cartilage topography, thickness, and contact areas from MRI: in-vitro calibration and in-vivo measurements. Osteoarthritis Cartilage. 1999; 7:95–109. [PubMed: 10367018]
26. Cohen ZA, Mow VC, Henry JH, Levine WN, Ateshian GA. Templates of the cartilage layers of the patellofemoral joint and their use in the assessment of osteoarthritic cartilage damage. Osteoarthritis Cartilage. 2003; 11:569–579. [PubMed: 12880579]
27. Cohen ZA, Roglic H, Grelsamer RP, et al. Patellofemoral stresses during open and closed kinetic chain exercises. An analysis using computer simulation. Am J Sports Med. 2001; 29:480–487. [PubMed: 11476390]
28. D'Lima DD, Chen PC, Kester MA, Colwell CW Jr. Impact of patellofemoral design on patellofemoral forces and polyethylene stresses. J Bone Joint Surg Am 85-A Suppl. 2003; 4:85–93.
29. Eckstein F, Sittek H, Milz S, Putz R, Reiser M. The morphology of articular cartilage assessed by magnetic resonance imaging (MRI). Reproducibility and anatomical correlation. Surg Radiol Anat. 1994; 16:429–438. [PubMed: 7725201]
30. Elliott DM, Narmoneva DA, Setton LA. Direct measurement of the Poisson's ratio of human patella cartilage in tension. J Biomech Eng. 2002; 124:223–228. [PubMed: 12002132]
31. Ewers BJ, Newberry WN, Haut RC. Chronic softening of cartilage without thickening of underlying bone in a joint trauma model. J Biomech. 2000; 33:1689–1694. [PubMed: 11006394]
32. Flatow EL, Ateshian GA, Soslowsky LJ, et al. Computer simulation of glenohumeral and patellofemoral subluxation. Estimating pathological articular contact. Clin Orthop. 1994:28–33. [PubMed: 8070206]
33. Forster H, Fisher J. The influence of continuous sliding and subsequent surface wear on the friction of articular cartilage. Proc Inst Mech Eng [H]. 1999; 213:329–345.
34. Forster H, Fisher J. The influence of loading time and lubricant on the friction of articular cartilage. Proc Inst Mech Eng [H]. 1996; 210:109–119.
35. Freed LE, Vunjak-Novakovic G, Biron RJ, et al. Biodegradable polymer scaffolds for tissue engineering. Biotechnology (N Y). 1994; 12:689–693. [PubMed: 7764913]
36. Froimson MI, Ratcliffe A, Gardner TR, Mow VC. Differences in patellofemoral joint cartilage material properties and their significance to the etiology of cartilage surface fibrillation. Osteoarthritis Cartilage. 1997; 5:377–386. [PubMed: 9536286]
37. Fukubayashi T, Kurosawa H. The contact area and pressure distribution pattern of the knee. A study of normal and osteoarthrotic knee joints. Acta Orthop Scand. 1980; 51:871–879. [PubMed: 6894212]
38. Fukui N, Ueno T, Fukuda A, Nakamura K. The use of stereolithography for an unusual patellofemoral disorder. Clin Orthop. 2003:169–174. [PubMed: 12671499]
39. Fulkerson JP. Anteromedialization of the tibial tuberosity for patellofemoral malalignment. Clin Orthop. 1983:176–181. [PubMed: 6861394]
40. Gandy SJ, Dieppe PA, Keen MC, et al. No loss of cartilage volume over three years in patients with knee osteoarthritis as assessed by magnetic resonance imaging. Osteoarthritis Cartilage. 2002; 10:929–937. [PubMed: 12464553]
41. Ghosh SK. A close-range photogrammetric system for 3-D measurements and perspective diagramming in biomechanics. J Biomech. 1983; 16:667–674. [PubMed: 6643539]
42. Gold GE, Besier TF, Draper CE, et al. Weight-bearing MRI of patellofemoral joint cartilage contact area. J Magn Reson Imaging. 2004; 20:526–530. [PubMed: 15332263]
43. Graichen H, von Eisenhart-Rothe R, Vogl T, Englmeier KH, Eckstein F. Quantitative assessment of cartilage status in osteoarthritis by quantitative magnetic resonance imaging: technical

validation for use in analysis of cartilage volume and further morphologic parameters. Arthritis Rheum. 2004; 50:811–816. [PubMed: 15022323]

44. Heino Brechter J, Powers CM, Terk MR, Ward SR, Lee TQ. Quantification of patellofemoral joint contact area using magnetic resonance imaging. Magn Reson Imaging. 2003; 21:955–959. [PubMed: 14684196]
45. Hills BA, Butler BD. Surfactants identified in synovial fluid and their ability to act as boundary lubricants. Ann Rheum Dis. 1984; 43:641–648. [PubMed: 6476922]
46. Huang CY, Mow VC, Ateshian GA. The role of flow-independent viscoelasticity in the biphasic tensile and compressive responses of articular cartilage. J Biomech Eng. 2001; 123:410–417. [PubMed: 11601725]
47. Huberti HH, Hayes WC. Contact pressures in chondromalacia patellae and the effects of capsular reconstructive procedures. J Orthop Res. 1988; 6:499–508. [PubMed: 3379503]
48. Huberti HH, Hayes WC. Patellofemoral contact pressures. The influence of q-angle and tendofemoral contact. J Bone Joint Surg Am. 1984; 66:715–724. [PubMed: 6725318]
49. Hudelmaier M, Glaser C, Hohe J, et al. Age-related changes in the morphology and deformational behavior of knee joint cartilage. Arthritis Rheum. 2001; 44:2556–2561. [PubMed: 11710712]
50. Huiskes R, Kremers J, de Lange A, et al. Analytical stereophotogrammetric determination of three-dimensional knee-joint geometry. J Biomech. 1985; 18:559–570. [PubMed: 4055811]
51. Hung CT, Lima EG, Mauck RL, et al. Anatomically shaped osteochondral constructs for articular cartilage repair. J Biomechanics. 2003; 36:1853–1864.
52. Hung CT, Mauck RL, Lima EG, Wang CC-B, Ateshian GA. A paradigm for functional tissue engineering of articular cartilage via applied physiologic deformational loading. Ann Biomed Eng. 2004; 32:35–49. [PubMed: 14964720]
53. Jeffrey JE, Gregory DW, Aspden RM. Matrix damage and chondrocyte viability following a single impact load on articular cartilage. Arch Biochem Biophys. 1995; 322:87–96. [PubMed: 7574698]
54. Kempson GE, Freeman MA, Swanson SA. Tensile properties of articular cartilage. Nature. 1968; 220:1127–1128. [PubMed: 5723609]
55. Kim YJ, Bonassar LJ, Grodzinsky AJ. The role of cartilage streaming potential, fluid flow and pressure in the stimulation of chondrocyte biosynthesis during dynamic compression. J Biomech. 1995; 28:1055–1066. [PubMed: 7559675]
56. Kisiday JD, Jin M, DiMicco MA, Kurz B, Grodzinsky AJ. Effects of dynamic compressive loading on chondrocyte biosynthesis in self-assembling peptide scaffolds. J Biomech. 2004; 37:595–604. [PubMed: 15046988]
57. Krishnan R, Kopacz M, Ateshian GA. Experimental verification of the role of interstitial fluid pressurization in cartilage lubrication. J Orthop Res. 2004; 22:565–570. [PubMed: 15099636]
58. Krishnan R, Park S, Eckstein F, Ateshian GA. Inhomogeneous cartilage properties enhance superficial interstitial fluid support and frictional properties, but do not provide a homogeneous state of stress. J Biomech Eng. 2003; 125:569–577. [PubMed: 14618915]
59. Lima EG, Mauck RL, Han SH, et al. Functional tissue engineering of chondral and osteochondral constructs. Biorheology. 2004; 41:577–590. [PubMed: 15299288]
60. Macirowski T, Tepic S, Mann RW. Cartilage stresses in the human hip joint. J Biomech Eng. 1994; 116:10–18. [PubMed: 8189704]
61. Malcom, LL. An experimental investigation of the frictional and deformational response of articular cartilage interfaces to static and dynamic loading. San Diego: University of California; 1976.
62. Maquet P. Advancement of the tibial tuberosity. Clin Orthop. 1976:225–230. [PubMed: 1253488]
63. Maquet P. Mechanics and osteoarthritis of the patellofemoral joint. Clin Orthop. 1979:70–73. [PubMed: 535253]
64. Mauck RL, Nicoll SB, Seyhan SL, Ateshian GA, Hung CT. Synergistic action of growth factors and dynamic loading for articular cartilage tissue engineering. Tiss Eng. 2003; 9:597–611.
65. Mauck RL, Soltz MA, Wang CC, et al. Functional tissue engineering of articular cartilage through dynamic loading of chondrocyte-seeded agarose gels. J Biomech Eng. 2000; 122:252–260. [PubMed: 10923293]

66. Mauck RL, Wang CC-B, Cheng Q, et al. Optimization of parameters for articular cartilage tissue engineering with deformational loading. Trans Orthop Res Soc. 2003; 28:305.

67. Mauck RL, Wang CC-B, Oswald ES, et al. Optimization of cell seeding density and nutrient supply for articular cartilage tissue engineering with deformational loading. Osteoarthritis and Cartilage. 2003; 11:879–890. [PubMed: 14629964]

68. McCutchen CW. The frictional properties of animal joints. Wear. 1962; 5:1–17.

69. Milentijevic D, Helfet DL, Torzilli PA. Influence of stress magnitude on water loss and chondrocyte viability in impacted articular cartilage. J Biomech Eng. 2003; 125:594–601. [PubMed: 14618918]

70. Minas T. Autologous chondrocyte implantation for focal chondral defects of the knee. Clin Orthop. 2001:S349–S361. [PubMed: 11603718]

71. Mizuno Y, Kumagai M, Mattessich SM, et al. Q-angle influences tibiofemoral and patellofemoral kinematics. J Orthop Res. 2001; 19:834–840. [PubMed: 11562129]

72. Moro-oka T, Matsuda S, Miura H, et al. Patellar tracking and patellofemoral geometry in deep knee flexion. Clin Orthop. 2002:161–168. [PubMed: 11795728]

73. Mow, VC.; Ateshian, GA. Lubrication and Wear of Diarthrodial Joints. In: Mow, VC.; Hayes, WC., editors. Basic orthopaedic biomechanics. 2nd ed. Philadelphia: Lippincott-Raven; 1997. p. 275-315.

74. Mow VC, Kuei SC, Lai WM, Armstrong CG. Biphasic creep and stress relaxation of articular cartilage in compression: Theory and experiments. J Biomech Eng. 1980; 102:73–84. [PubMed: 7382457]

75. Mow VC, Lai WM. Recent developments in synovial joint biomechanics. SIAM Review. 1980; 22:275–317.

76. Obradovic B, Meldon JH, Freed LE, Vunjak-Novakovic G. Glycosaminoglycan deposition in engineered cartilage: experiments and mathematical model. AIChE J. 2000; 46:1860–1871.

77. Oloyede A, Broom ND. Is classical consolidation theory applicable to articular cartilage deformation? Clinical Biomechanics. 1991; 6:206–212. [PubMed: 23915565]

78. Park S, Hung CT, Ateshian GA. Mechanical response of bovine articular cartilage under dynamic unconfined compression loading at physiological stress levels. Osteoarthritis and Cartilage. 2004; 12:65–73. [PubMed: 14697684]

79. Park S, Krishnan R, Nicoll SB, Ateshian GA. Cartilage interstitial fluid load support in unconfined compression. J Biomech. 2003; 36:1785–1796. [PubMed: 14614932]

80. Patel VV, Hall K, Ries M, et al. Magnetic resonance imaging of patellofemoral kinematics with weight-bearing. J Bone Joint Surg Am. 2003; 85-A:2419–2424. [PubMed: 14668513]

81. Peterfy CG, van Dijke CF, Janzen DL, et al. Quantification of articular cartilage in the knee with pulsed saturation transfer subtraction and fat-suppressed MR imaging: optimization and validation. Radiology. 1994; 192:485–491. [PubMed: 8029420]

82. Piazza SJ, Delp SL. Three-dimensional dynamic simulation of total knee replacement motion during a step-up task. J Biomech Eng. 2001; 123:599–606. [PubMed: 11783731]

83. Powers CM, Lilley JC, Lee TQ. The effects of axial and multi-plane loading of the extensor mechanism on the patellofemoral joint. Clin Biomech (Bristol, Avon). 1998; 13:616–624.

84. Puelacher WC, Kim SW, Vacanti JP, et al. Tissue-engineered growth of cartilage: the effect of varying the concentration of chondrocytes seeded onto synthetic polymer matrices. Int J Oral Maxillofac Surg. 1994; 23:49–53. [PubMed: 8163862]

85. Quinn TM, Allen RG, Schalet BJ, Perumbuli P, Hunziker EB. Matrix and cell injury due to sub-impact loading of adult bovine articular cartilage explants: effects of strain rate and peak stress. J Orthop Res. 2001; 19:242–249. [PubMed: 11347697]

86. Radin EL, Swann DA, Weisser PA. Separation of a hyaluronate-free lubricating fraction from synovial fluid. Nature. 1970; 228:377–378. [PubMed: 5473985]

87. Raynauld JP, Martel-Pelletier J, Berthiaume MJ, et al. Quantitative magnetic resonance imaging evaluation of knee osteoarthritis progression over two years and correlation with clinical symptoms and radiologic changes. Arthritis Rheum. 2004; 50:476–487. [PubMed: 14872490]

88. Sah RL, Kim YJ, Doong JY, et al. Biosynthetic response of cartilage explants to dynamic compression. J Orthop Res. 1989; 7:619–636. [PubMed: 2760736]

89. Salsich GB, Ward SR, Terk MR, Powers CM. In vivo assessment of patellofemoral joint contact area in individuals who are pain free. Clin Orthop. 2003:277–284. [PubMed: 14646727]

90. Schaefer D, Martin I, Shastri P, et al. In vitro generation of osteochondral composites. Biomaterials. 2000; 21:2599–2606. [PubMed: 11071609]

91. Schinagl RM, Gurskis D, Chen AC, Sah RL. Depth-dependent confined compression modulus of full-thickness bovine articular cartilage. J Orthop Res. 1997; 15:499–506. [PubMed: 9379258]

92. Sittek H, Eckstein F, Gavazzeni A, et al. Assessment of normal patellar cartilage volume and thickness using MRI: an analysis of currently available pulse sequences. Skeletal Radiol. 1996; 25:55–62. [PubMed: 8717120]

93. Sittinger M, Bujia J, Minuth WW, Hammer C, Burmester GR. Engineering of cartilage tissue using bioresorbable polymer carriers in perfusion culture. Biomaterials. 1994; 15:451–456. [PubMed: 8080936]

94. Soltz MA, Ateshian GA. A Conewise Linear Elasticity mixture model for the analysis of tension-compression nonlinearity in articular cartilage. J Biomech Eng. 2000; 122:576–586. [PubMed: 11192377]

95. Soltz MA, Ateshian GA. Experimental verification and theoretical prediction of cartilage interstitial fluid pressurization at an impermeable contact interface in confined compression. J Biomech. 1998; 31:927–934. [PubMed: 9840758]

96. Soltz MA, Ateshian GA. Interstitial fluid pressurization during confined compression cyclical loading of articular cartilage. Ann Biomed Eng. 2000; 28:150–159. [PubMed: 10710186]

97. Soulhat J, Buschmann MD, Shirazi-Adl A. A fibril-network-reinforced biphasic model of cartilage in unconfined compression. J Biomech Eng. 1999; 121:340–347. [PubMed: 10396701]

98. Staubli HU, Durrenmatt U, Porcellini B, Rauschning W. Anatomy and surface geometry of the patellofemoral joint in the axial plane. J Bone Joint Surg Br. 1999; 81:452–458. [PubMed: 10872365]

99. Swann DA, Hendren RB, Radin EL, Sotman SL, Duda EA. The lubricating activity of synovial fluid glycoproteins. Arthritis Rheum. 1981; 24:22–30. [PubMed: 7470168]

100. Torzilli PA, Grigiene R, Borrelli J Jr. Helfet DL. Effect of impact load on articular cartilage: cell metabolism and viability, and matrix water content. J Biomech Eng. 1999; 121:433–441. [PubMed: 10529909]

101. van Kampen A, Huiskes R. The three-dimensional tracking pattern of the human patella. J Orthop Res. 1990; 8:372–382. [PubMed: 2324856]

102. Wiberg G. Roentgenographic and anatomic studies on the femoro-patellar joint: with special reference to chondromalacia patellae. Acta Orthop Scand. 1941; 12:319–410.

103. Yates JW Jr. The effectiveness of autologous chondrocyte implantation for treatment of full-thickness articular cartilage lesions in workers' compensation patients. Orthopedics. 2003; 26:295–300. discussion 300–291. [PubMed: 12650322]

104. Zarek JM, Edward J. The stress-structure relationship in articular cartilage. Med Electron Biol Eng. 1963; 1:497–507.

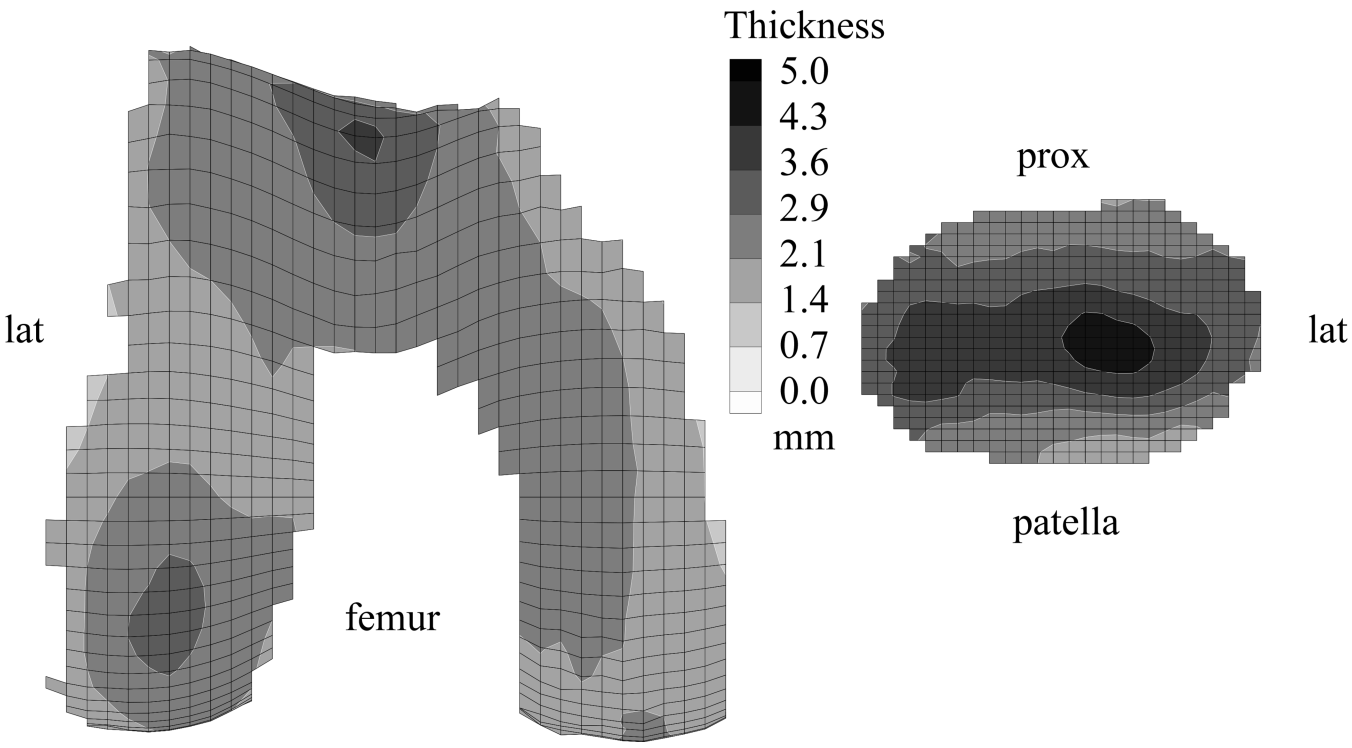

Fig 1.

Average cartilage thickness maps for the femoral and patellar surfaces of 14 non-arthritic patellofemoral joints are shown. Reprinted with permission from Cohen ZA, Mow VC, Henry JH, Levine WN, Ateshian GA: Templates of the cartilage layers of the patellofemoral joint and their use in the assessment of osteoarthritic cartilage damage. Osteoarthritis Cartilage 11:569–579, 2003.

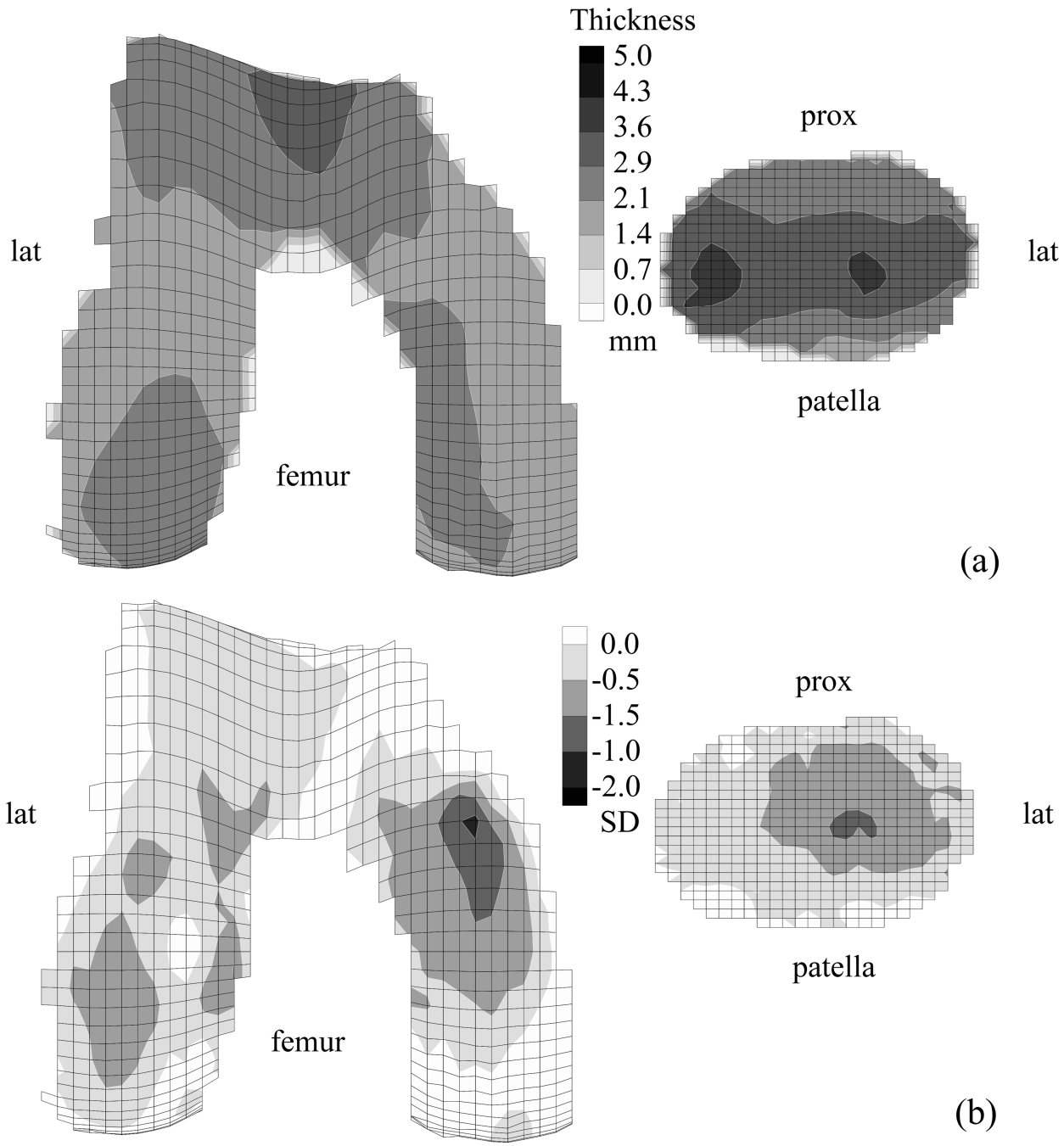

Fig 2.

A–B. Average cartilage thickness maps for the femoral and patellar surfaces of 33 knees with patellofemoral joint OA are shown. (A) The mean cartilage thickness map, plotted on mean articular surface topography of OA joints is shown. (B) The difference maps against the normal template, scaled by the local standard deviation of normal cartilage thickness, and plotted on the articular surface topography from the normal template are shown. Darker regions indicate regions of cartilage loss. Reprinted with permission from Cohen ZA, Mow VC, Henry JH, Levine WN, Ateshian GA: Templates of the cartilage layers of the patellofemoral joint and their use in the assessment of osteoarthritic cartilage damage. Osteoarthritis Cartilage 11:569–579, 2003.

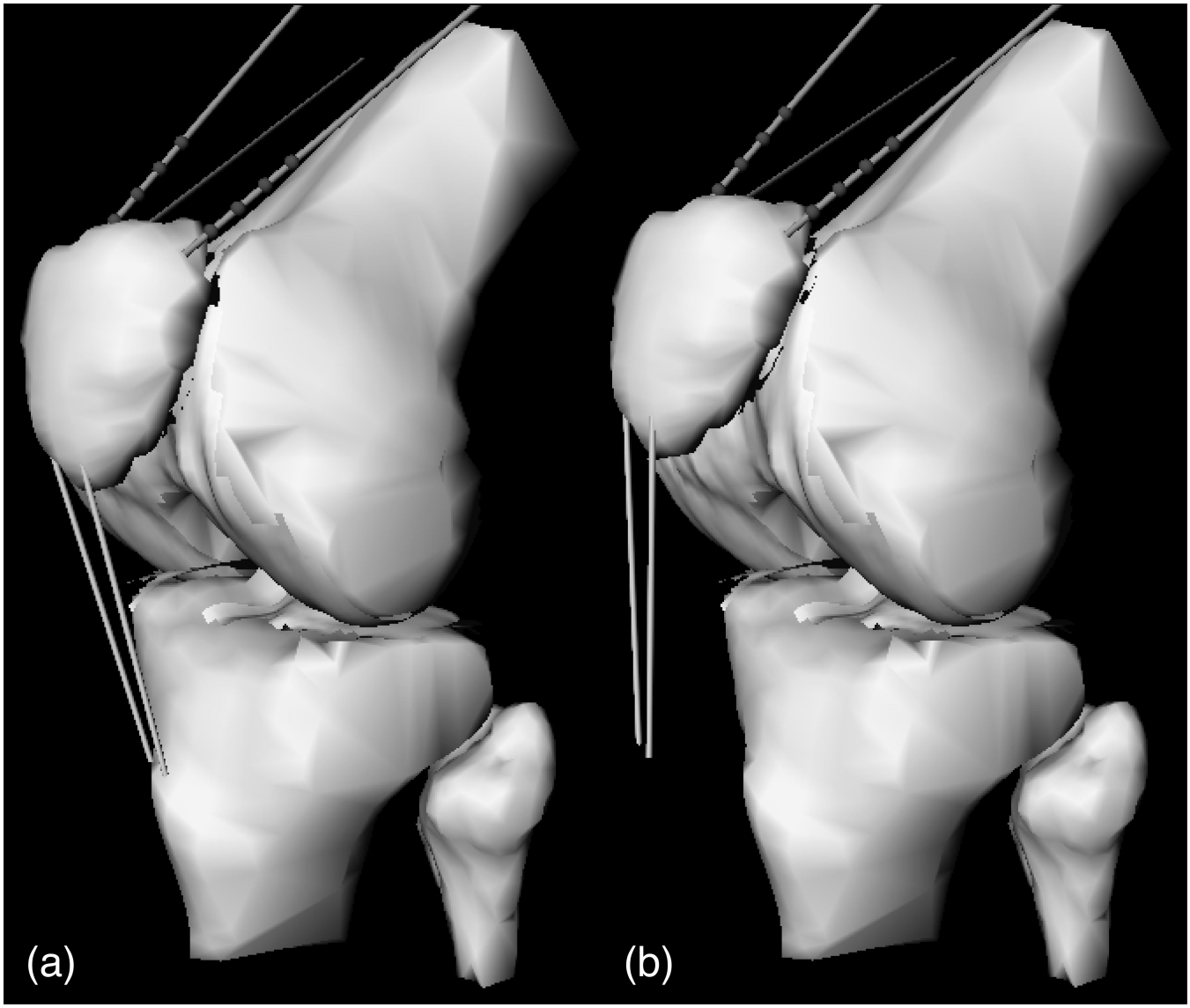

Fig 3.
A–B. A physics-based model of the knee of a patient with PFJ osteoarthritis. The (A) original model and (B) the model with simulated 20 mm of tuberosity transfer are shown.[24]

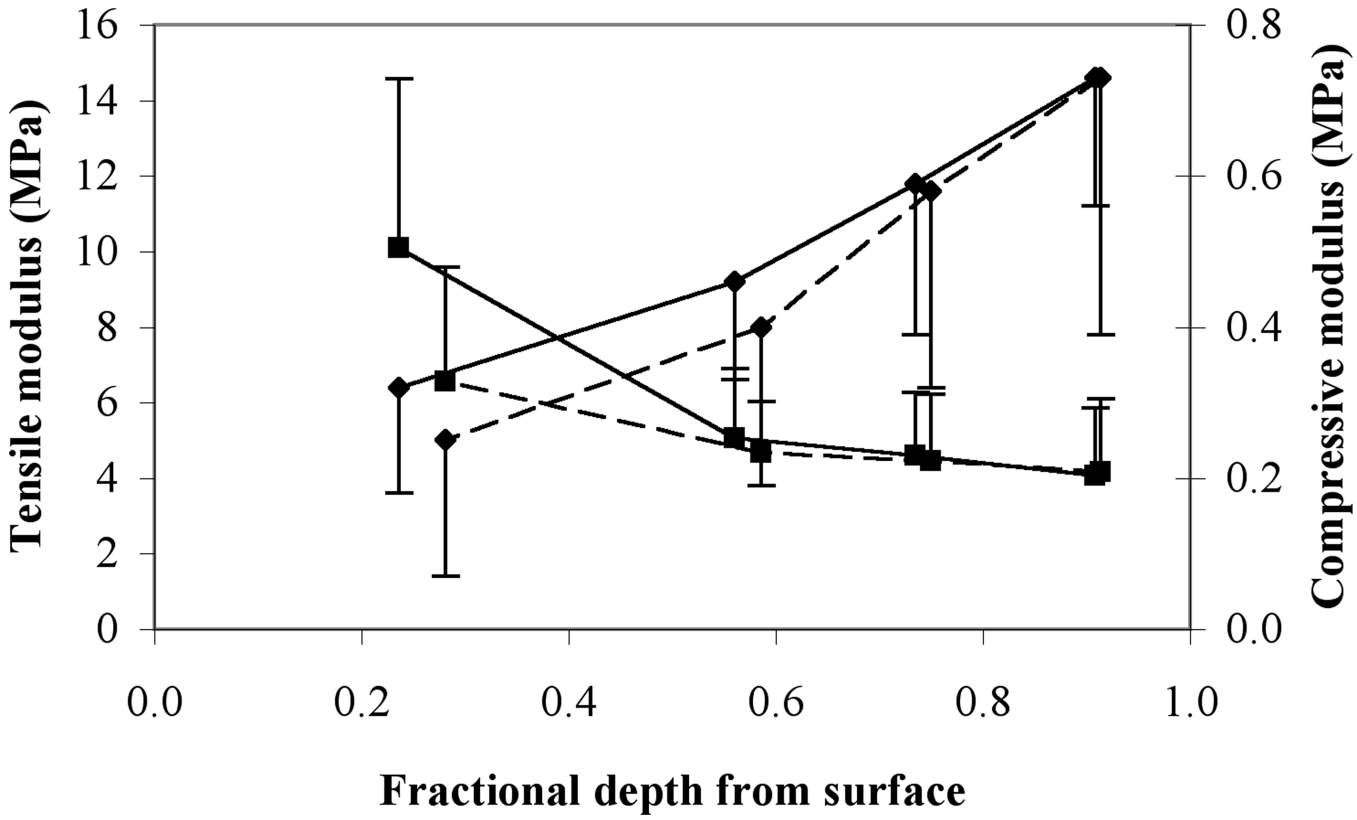

Fig 4.

Mean and standard deviation of equilibrium tensile (square symbol) and compressive (diamond) moduli of human patellar (dashed line) and femoral (solid line) cartilage as a function of depth from the articular surface are shown. Results are from 4 men and 2 women, aged 45.5±12.0 years.[58]

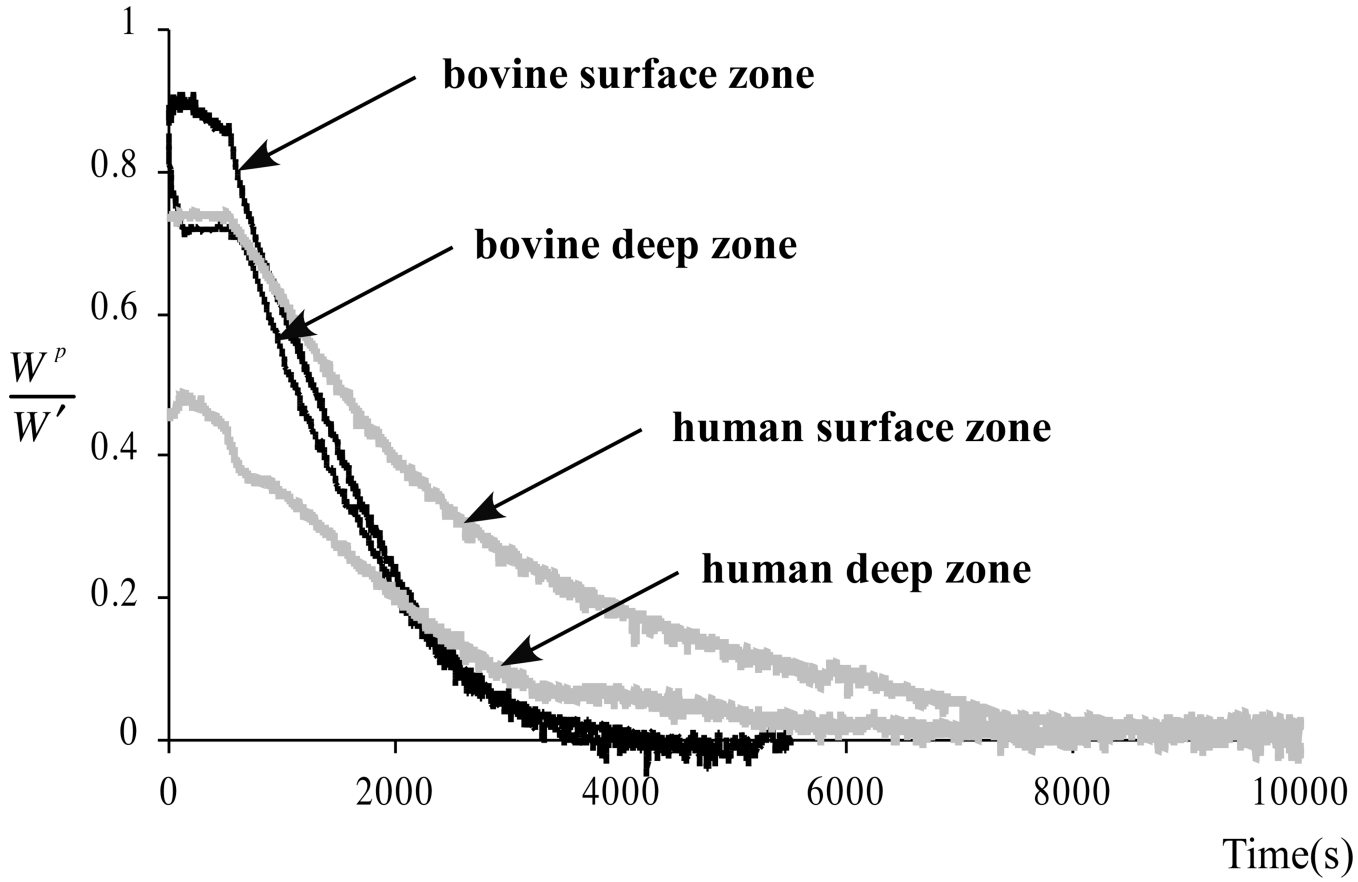

Fig 5.

Experimental measurements of interstitial fluid load support (W^p = load supported by fluid pressure, W = total applied load) in unconfined compression stress-relaxation of cylindrical disks of human and bovine cartilage are shown. The fluid load support is higher at the articular surface, where the ratio of tensile to compressive modulus is greatest. Reprinted with permission from Park S, Krishnan R, Nicoll SB, Ateshian GA: Cartilage interstitial fluid load support in unconfined compression. J Biomech 36:1785–1796, 2003.

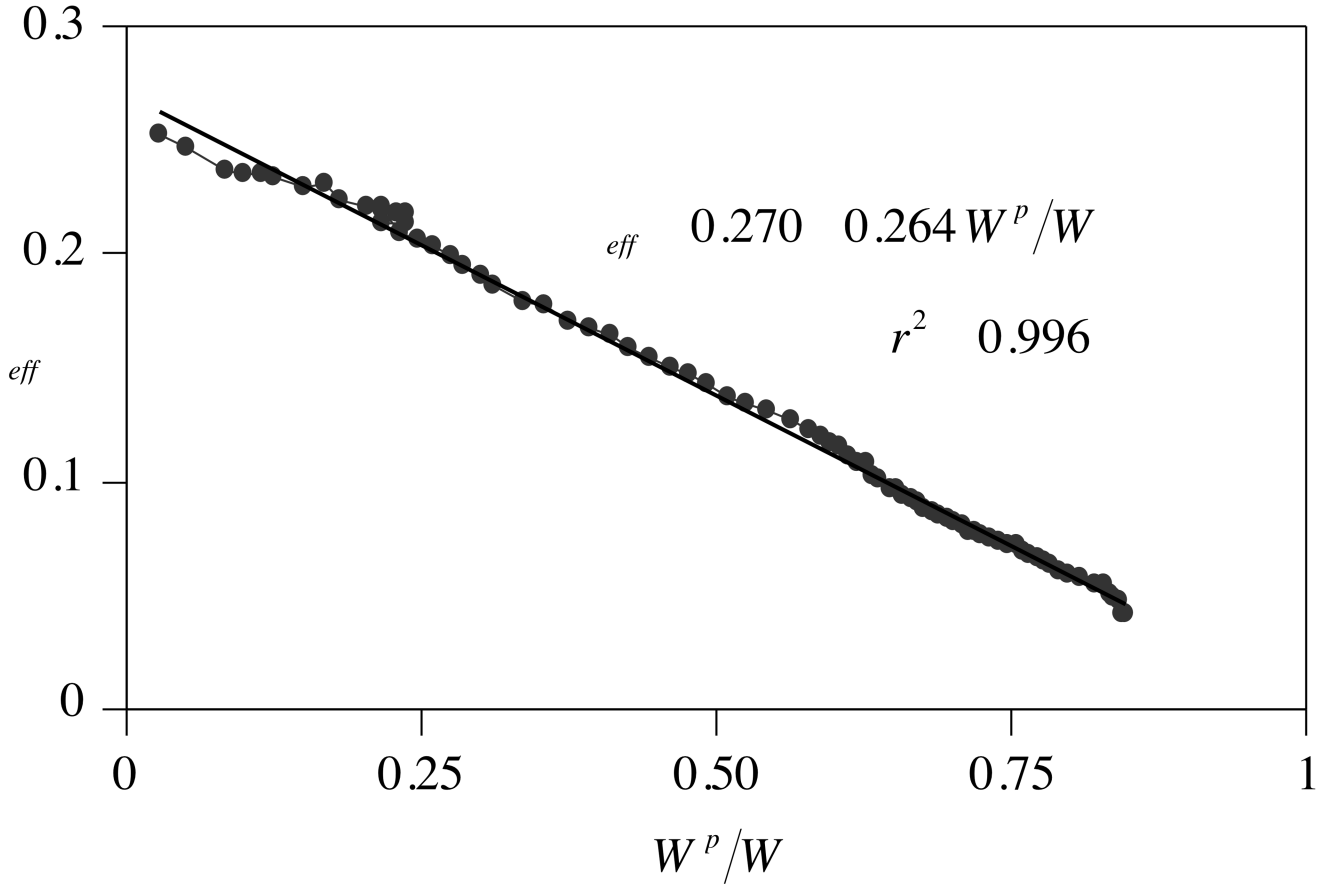

Fig 6.
Cartilage friction coefficient, μ_{eff}, versus interstitial fluid load support, W^p/W, during unconfined compression creep of a cylindrical bovine cartilage disk is shown. The μ_{eff} achieves its lowest value when W^p/W is greatest. Reprinted with permission from Krishnan R, Kopacz M, Ateshian GA: Experimental verification of the role of interstitial fluid pressurization in cartilage lubrication. J Orthop Res 22:565–570, 2004.

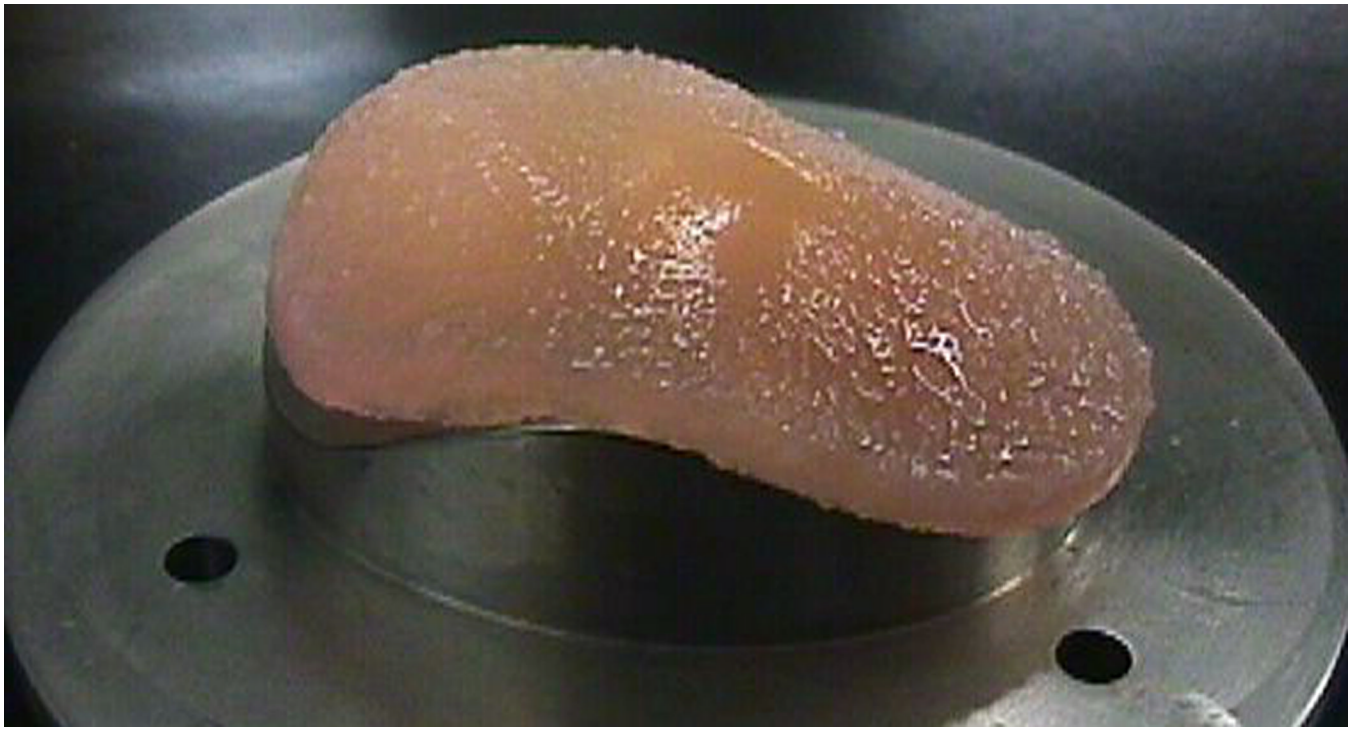

Fig 7.

A tissue-engineered cartilage construct in the shape of a human patellar cartilage layer, at day 35 of free-swelling culture is shown; the bottom platen is one of the two molds used for casting the chondrocyte-seeded agarose gel in the desired shape. Reprinted with permission from Hung CT, Lima EG, Mauck RL, et al: Anatomically shaped osteochondral constructs for articular cartilage repair. J Biomechanics 36:1853–1864, 2003.

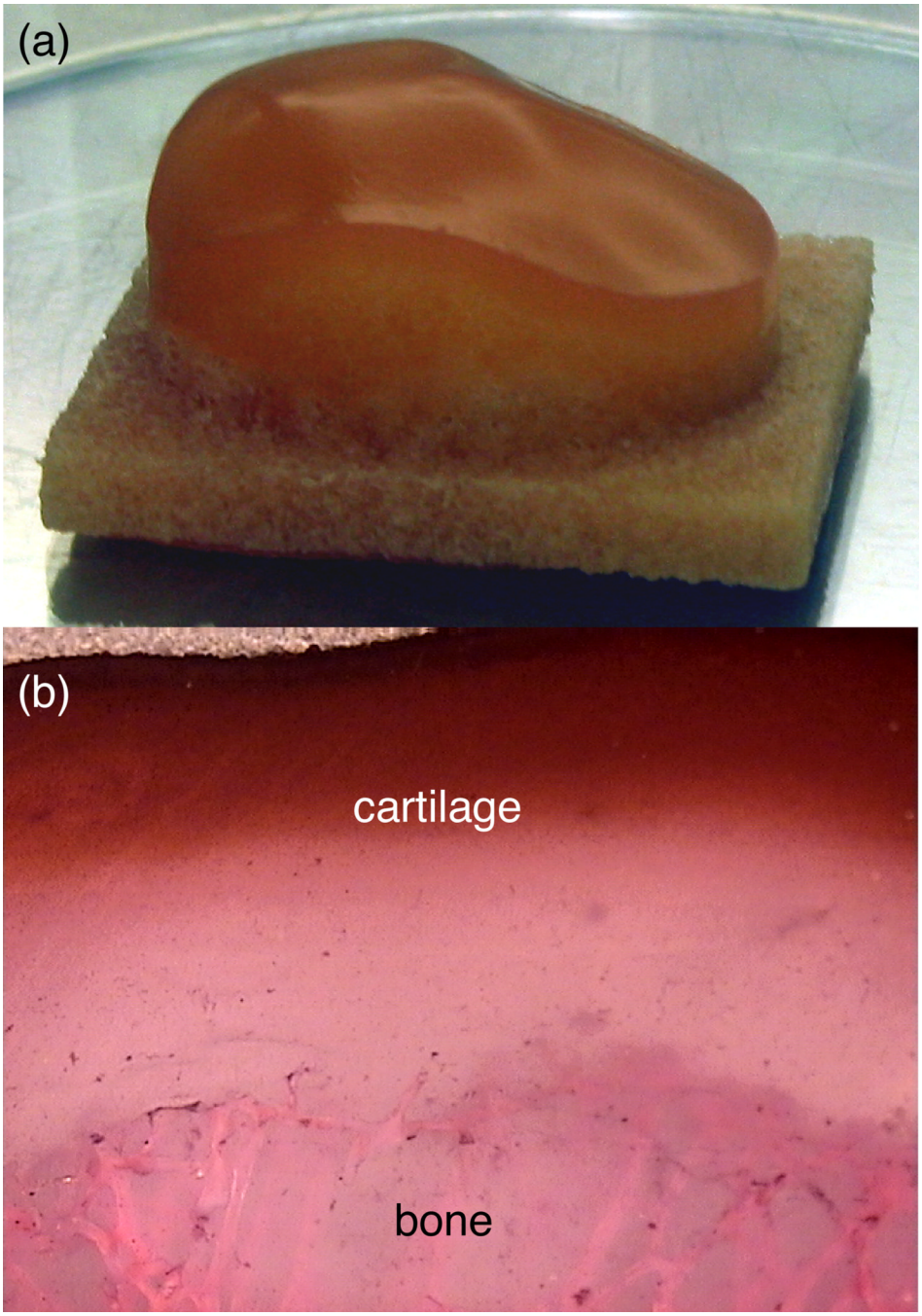

Fig 8.

A–B. (A) Osteochondral patellar constructs, using bovine trabecular bone as the substrate, are shown. (B) A section of osteochondral construct after 35 days of free-swelling culture shows GAG distribution (stain, Safranin-O; magnification 4×).[52]